Supplementary Information

Synthesis, screening and sensing applications of a novel fluorescent probe based on C-glycosides

Tao Zhang, Tianyi Wang, Zhijie Fang*

Department of Chemical Engineering, Nanjing University of Science and Technology, Nanjing 210094, P. R. China.

Contents of Supplementary Information:

1. Density functional theory (DFT) calculations of arylvinyl ketone C-furyl glycosides 3a-3h

Energy-optimized structures of **3a-3h** were obtained with the Gaussian 03 package at the B3LYP/6-31g* level. The energies of virtual orbitals, as well as the energy gap (Eg) between the highest occupied molecular orbital (HOMO) and the lowest unoccupied molecular orbital (LUMO) of **3a-3h** were also obtained by DFT method and shown in Figure S1. The electronic structure calculations show that the values of Eg are in the range of 3.53-4.10eV, with compound **3h** having the lowest Eg value. Increasing the electron-donating character and the conjugation extent of the system enhances both HOMO and LUMO energy levels. Consequently, the Eg value of **3h** bearing a terminal diethylamine moiety is lower than that of **3b**, **3c** and **3e** with dimethylamine, methoxyl and methyl groups, respectively. Comparing **3h** with its analogs **3f** and **3g** in which the spacers provide elongated π-conjugations with naphthalene and cinnamaldehyde, we can see that the energies of HOMO increase and the Eg values decrease in the order of **3h**, **3g** and **3f**. Moreover, the emission wavelength shows a trend towards bathochromic shift, when comparing **3h** (518nm) and **3b** (510nm).

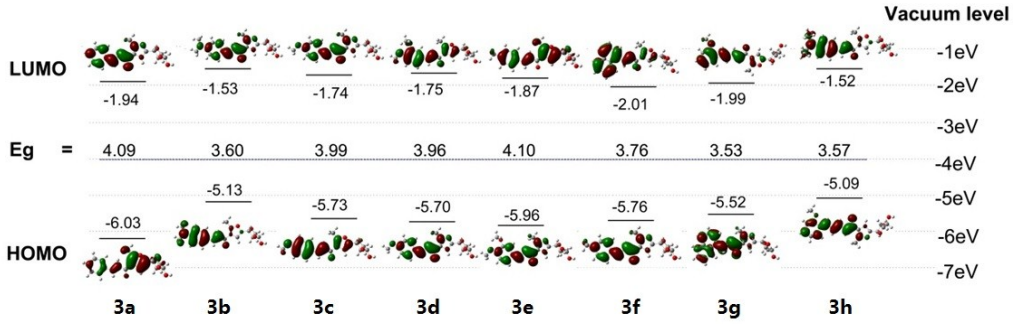

Figure S1. HOMO and LUMO orbitals analysis of 3a-3h

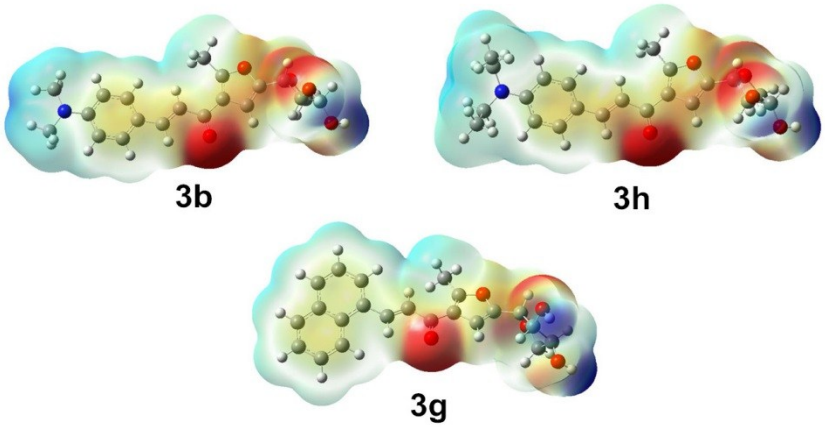

Figure S2. Computed electrostatic potential on the 0.001 a.u. molecular surface at B3LPY/6-31g* level, with values -0.04 to 0.04 a.u. Color coding: red, negative; yellow, slightly negative; green, neutral; light blue, slightly positive; dark blue, positive.

2. Fluorescence detection of trypsin

The activity of enzymes can be affected by various factors such as temperature, interfering ions, presence of inhibitors, etc. Based on the high sensitivity and ease of use, fluorescence measurement was selected for studying the change in activity of the trypsin enzyme. Figure S3(a) shows the dependence of the intensity ratio of the dye-BSA complex on the concentration of trypsin. In the absence of trypsin, the fluorescence intensity of the dye-BSA complex remained unchanged. After addition of trypsin, the fluorescence intensity decreased gradually. The increase of amount of added trypsin results in high initial cleavage reaction rates, thus showing a marked change in the fluorescence. Figure S3(b) shows the plot of the rate of enzymolysis at different temperatures. The enzymolysis was studied at different testing temperatures of 288K, 298K and 310K. At the optimum temperature of 310K, the intensity decreased most rapidly and the enzymolysis reaction reached the maximum speed.

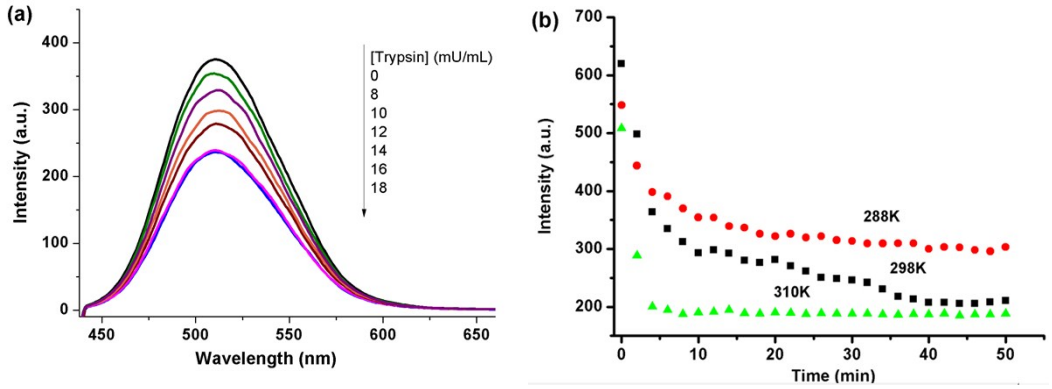

Figure S3. (a) Fluorescence spectra of the dye-BSA (10μM and 1.6mg/mL) complex in the presence of different concentrations of trypsin. (b) The speed of enzymolysis at different temperatures, Slit (3, 1.5).

3. Fluorescence imaging of cells in the presence of dye 3h

In vitro experiments were performed using A549 cell. The cell was cultured in complete DMEM (high glucose) medium in an atmosphere of 5% CO_2 at 37 ^oC. Before staining, cells were incubated with dye 3h 100 nM for 1h at room temperature. The fluorescence imaging of cells was observed under a Nikon H550L fluorescence microscopy equipped with a Nikon DS-Ril imaging system (excited with green light). The fluorescence microscopic studies indicated that the cells were stained and generated strong green fluorescence, as shown in Figure S4. Therefore, a potential “turn-on” probe with good sensitivity and strong fluorescence has been developed here for cytology experiments.

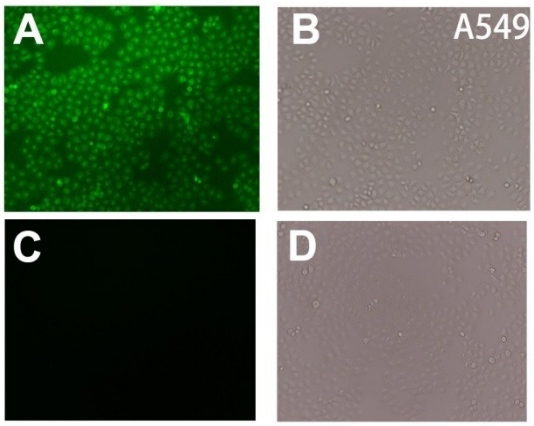

Figure S4. Microscopy fluorescence imaging of A549 cells incubated with dye **3h**. The cells were incubated with 100nM **3h** for 1h at room temperature. (A) Fluorescence image of A549 cells after incubation with dye **3h**. (B) Bright-field image. (C) Fluorescence image of A549 cells before incubation with dye **3h**. (D) Bright-field image. Scale bar, 100μm.

4. Spectra analysis of compound 3h, A and B.

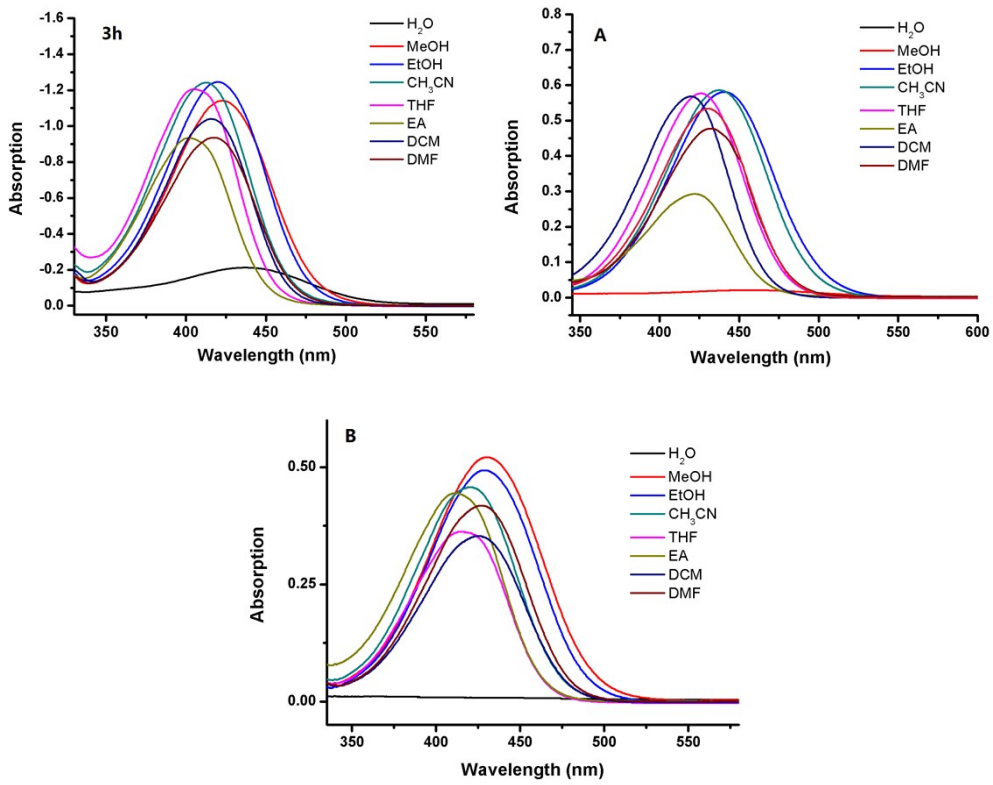

Figure S5. Solvents impacts to UV detection of compound **3h**, **A** and **B** (10μM).

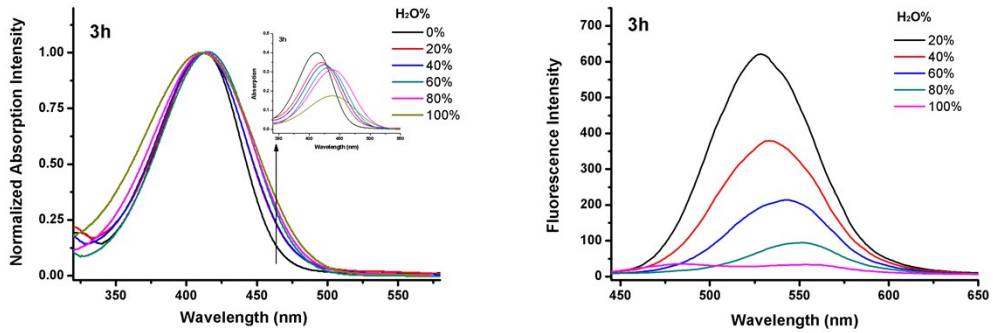

Figure S6. Normalized absorption spectra and fluorescence spectra of compound **3h** (10μM) in the mixture of acetonitrile and water. Slit (5, 3).

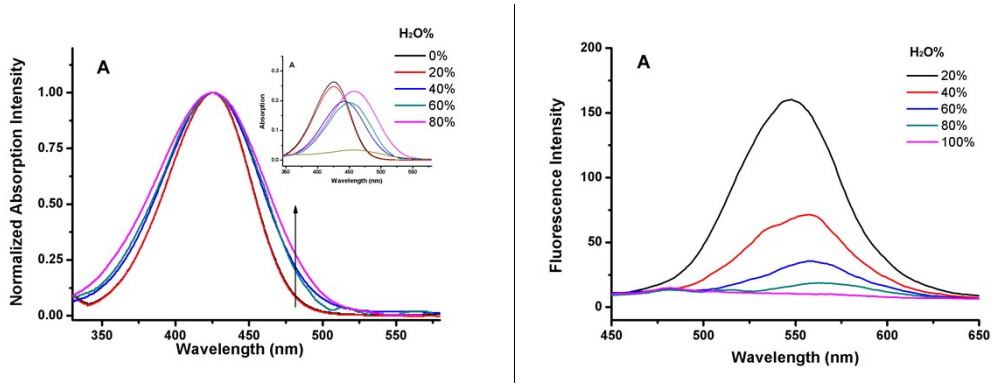

Figure S7. Normalized absorption spectra and fluorescence spectra of compound **A** (10μM) in the mixture of acetonitrile and water. Slit (5, 3).

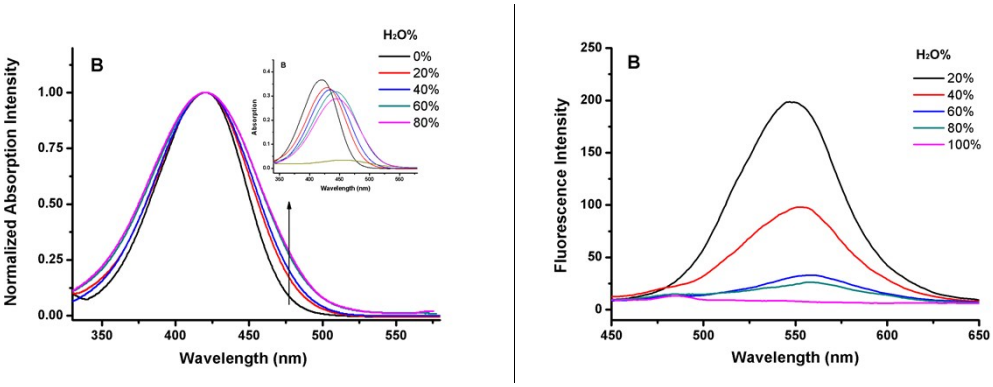

Figure S8. Normalized absorption spectra and fluorescence spectra of compound **B** (10μM) in the mixture of acetonitrile and water. Slit (5, 3).

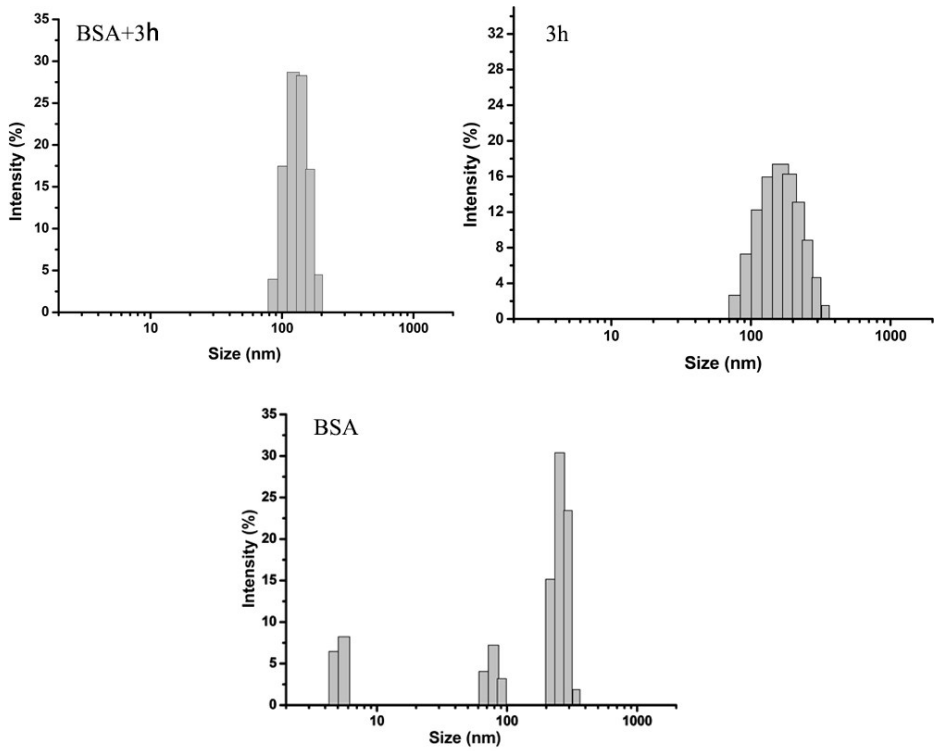

Figure S9. The schematic of dynamic light scattering measurement for BSA+**3h**, **3h** and BSA. 25°C, solvent: water. 3h: 40μM, BSA: 1.6mg/mL.

Table S1. Spectral data of **3h** in different solvents.

Solvents	Abs./ Em.(nm)	Stokes Shift(nm)	Abs. (nm)	Φ
DMF	419/502	83	0.935	0.28
Acetonitrile	413/518	100	1.242	0.24
DCM	415/498	83	1.04	0.20
THF	405/479	74	1.205	0.11
Ethyl acetate	402/480	78	0.934	0.24
Ethanol	420/529	109	1.246	0.060
Methanol	423/534	111	1.142	0.027
Water	437/549	112	0.213	0.0027

5. Characterization of arylvinyl ketone C-furyl glycosides 3a-3h

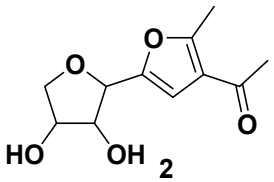

2

Compound 2: obtained in 87% yield; yellow powder; ^{1}H NMR (300 MHz, $CDCl_3$) δ 6.57 (s, 1H), 4.61 (d, *J* = 6.2 Hz, 1H), 4.32 (t, *J* = 4.6 Hz, 2H), 4.19 (dd, *J* = 10.0, 4.3 Hz, 1H), 3.85 (dd, *J* = 13.0, 3.7 Hz, 2H), 3.76 (s, 1H), 2.52 (s, 3H), 2.34 (s, 3H). ^{13}C NMR (126 MHz, $CDCl_3$): δ 193.9, 158.2, 149.2, 121.1, 108.4, 75.9, 73.7, 72.1, 70.0, 28.1, 13.6. MS (ESI +C): $[M + Na]^+$, 249.1. Elemental Anal. Found: C (58.21%) H (6.38%) Calcd for $C_{22}H_{28}O_8$ = C (58.40%) H (6.24%).

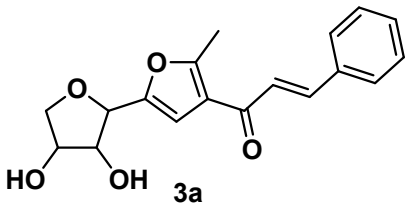

3a

Compound 3a: obtained in 82% yield; yellow oil; ^{1}H NMR (500 MHz, $CDCl_3$) δ 7.71 (d, *J* = 15.7 Hz, 1H), 7.59 (dd, *J* = 6.6, 2.9 Hz, 2H), 7.41 (dd, *J* = 6.3, 3.6 Hz, 3H), 7.16 (d, *J* = 15.7 Hz, 1H), 6.74 (s, 1H), 4.71 (d, *J* = 6.3 Hz, 1H), 4.42 (t, *J* = 4.9 Hz, 2H), 4.27 (dd, *J* = 10.0, 4.7 Hz, 1H), 3.92 (dd, *J* = 10.2, 2.4 Hz, 1H), 3.53 (s, 1H), 3.28 (s, 1H), 2.62 (s, 3H). ^{13}C NMR (126 MHz, $CDCl_3$): δ 186.1, 160.0, 150.1, 143.7, 134.5, 130.5, 129.1, 128.9, 128.4, 123.6, 122.3, 109.1, 76.9, 74.7, 73.1, 71.0, 14.1. HRMS (ESI) m/z: calcd for $C_{18}H_{18}O_5$ $[M + H]^+$ 315.1232, found 315.1226.

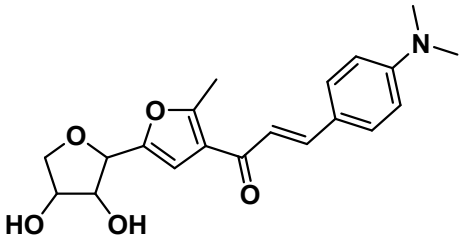

3b

Compound 3b: obtained in 92% yield; orange powder; mp 128.0-128.5 °C; ^{1}H NMR (300 MHz, $CDCl_3$) δ 7.68 (d, *J* = 15.5 Hz, 1H), 7.49 (d, *J* = 8.8 Hz, 2H), 6.95 (d, *J* = 15.5 Hz, 1H), 6.77 – 6.60 (m, 3H), 4.48 – 4.34 (m, 2H), 4.32 – 4.20 (m, 1H), 3.91 (dd, *J* = 10.1, 2.1 Hz, 1H), 3.03 (s, 7H), 2.60 (s, 3H). ^{13}C NMR (75 MHz, $CDCl_3$): δ 186.1, 159.2, 152.0, 149.6, 144.6, 130.3, 122.6, 122.3, 118.5, 111.8, 109.3, 77.2, 74.6, 73.2, 71.0, 40.0, 14.5. HRMS (ESI) m/z: calcd for $C_{20}H_{23}NO_5$ $[M + H]^+$ 358.1654, found 358.1648.

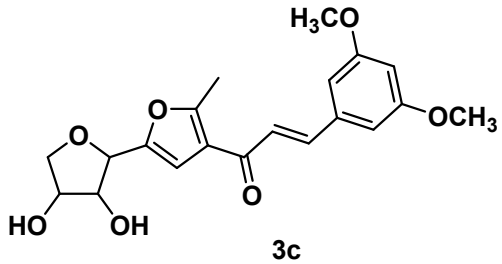

3c

Compound 3c: obtained in 90% yield; yellow powder; mp 120.3-120.7 ˚C; ^{1}H NMR (500 MHz, CDCl3) δ 7.61 (d, *J* = 15.7 Hz, 1H), 7.11 (d, *J* = 15.7 Hz, 1H), 6.75 – 6.69 (m, 3H), 6.51 (s, 1H), 4.69 (d, *J* = 6.5 Hz, 1H), 4.40 (dt, *J* = 11.9, 4.3 Hz, 2H), 4.27 (dd, *J* = 10.1, 4.6 Hz, 1H), 3.91 (dd, *J* = 10.1, 2.7 Hz, 1H), 3.82 (s, 6H), 2.62 (s, 3H). ^{13}C NMR (75 MHz, CDCl3): δ 185.8, 161.0, 160.1, 149.9, 143.5, 136.5, 124.1, 122.2, 109.1, 106.3, 102.6, 74.7, 73.2, 70.9, 55.4, 14.6. HRMS (ESI) m/z: calcd for $C_{20}H_{22}O_7$ $[M + H]^+$ 375.1444, found 375.1437.

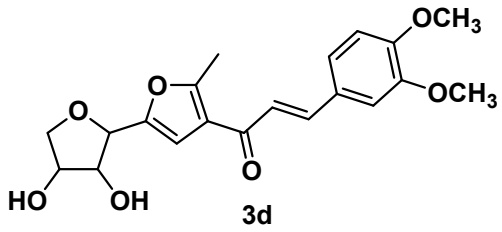

3d

Compound 3d: obtained in 85% yield; orange oil; ^{1}H NMR (500 MHz, $CDCl_3$) δ 7.64 – 7.56 (m, 1H), 7.17 – 7.10 (m, 1H), 7.07 (s, 1H), 6.99 (d, *J* = 15.6 Hz, 1H), 6.82 (d, *J* = 8.3 Hz, 1H), 6.71 (s, 1H), 5.00 (s, 2H), 4.67 (d, *J* = 4.0 Hz, 1H), 4.36 (d, *J* = 4.3 Hz, 2H), 4.26 – 4.16 (m, 1H), 3.96 – 3.71 (m, 9H), 2.55 (s, 3H). ^{13}C NMR (75 MHz, $CDCl_3$): δ 186.1, 159.7, 151.4, 149.9, 149.1, 143.9, 127.5, 123.2, 122.4, 121.5, 111.0, 109.2, 74.7, 73.1, 71.0, 55.9, 14.5. HRMS (ESI) m/z: calcd for $C_{20}H_{22}O_7$ $[M + H]^+$ 375.1444, found 375.1438.

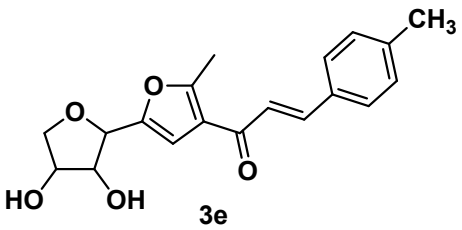

3e

Compound 3e: obtained in 87% yield; yellow powder; mp 124.2-125.6 ˚C; ^{1}H NMR (300 MHz, $CDCl_3$) δ 7.68 (d, *J* = 15.7 Hz, 1H), 7.48 (d, *J* = 8.0 Hz, 2H), 7.18 (d, *J* = 8.0 Hz, 2H), 7.12 (d, *J* = 15.7 Hz, 1H), 6.72 (s, 1H), 4.41 (s, 2H), 4.31 – 4.16 (m, 1H), 3.96 – 3.84 (m, 1H), 3.52 (s, 1H), 3.21 (s, 1H), 2.60 (s, 3H), 2.37 (s, 3H). ^{13}C NMR (75 MHz, $CDCl_3$): δ 186.0, 159.9, 149.9, 143.7, 141.1, 131.8, 129.6, 128.4, 122.6, 122.3, 109.1, 74.7, 73.2, 71.0, 21.4, 14.6. HRMS (ESI) m/z: calcd for $C_{19}H_{20}O_5$ $[M + H]^+$ 329.1389, found 329.1392.

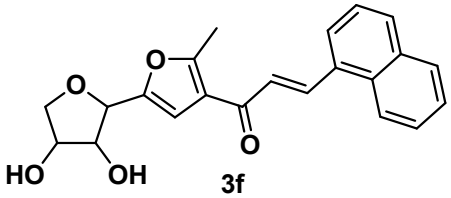

3f

Compound 3f: obtained in 76% yield; orange powder; mp 123.1-123.9 ˚C; ^{1}H NMR (500 MHz, $CDCl_3$) δ 8.57 (d, *J* = 15.4 Hz, 1H), 8.24 (d, *J* = 8.4 Hz, 1H), 7.89 (dd, *J* = 13.9, 8.1 Hz, 2H), 7.81 (d, *J* = 7.1 Hz, 1H), 7.55 (dt, *J* = 14.9, 6.9 Hz, 2H), 7.50 – 7.42 (m, 1H), 7.29 – 7.20 (m, 1H), 6.76 (s, 1H), 4.71 (d, *J* = 6.2 Hz, 1H), 4.49 – 4.38 (m, 2H), 4.28 (dd, *J* = 10.1, 2.5 Hz, 1H), 3.92 (dd, *J* = 10.3, 1.9 Hz, 1H), 3.32 (d, *J* = 55.9 Hz, 1H), 3.07 (s, 1H). ^{13}C NMR (75 MHz, $CDCl_3$): δ 185.7, 160.3, 150.0, 140.4, 130.8, 128.7, 126.9, 126.2, 125.3, 124.9, 109.1, 74.7, 73.2, 71.0, 14.7. HRMS (ESI) m/z: calcd for $C_{22}H_{20}O_5$ $[M + H]^+$ 365.1389, found 365.1379.

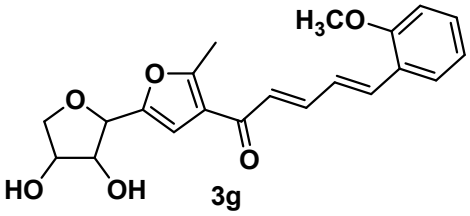

3g

Compound 3g: obtained in 83% yield; orange oil; ^{1}H NMR (500 MHz, $CDCl_3$) δ 7.47 (dd, *J* = 16.6, 9.2 Hz, 1H), 7.35 – 7.20 (m, 1H), 7.02 – 6.80 (m, 2H), 6.65 (t, *J* = 7.4 Hz, 1H), 4.69 (d, *J* = 5.8 Hz, 1H), 4.36 (d, *J* = 4.2 Hz, 1H), 4.19 (dd, *J* = 9.5, 3.6 Hz, 1H), 4.01 (dd, *J* = 34.4, 25.6 Hz, 2H), 3.92 – 3.74 (m, 3H), 2.55 (s, 2H). ^{13}C NMR (75 MHz, $CDCl_3$): δ 186.3, 159.6, 157.5, 150.0, 145.0, 137.4, 130.4, 127.5, 127.1, 126.3, 124.9, 122.4, 120.7, 111.0, 109.2, 76.8, 74.7, 73.0, 71.0, 55.4, 14.6. HRMS (ESI) m/z: calcd for $C_{21}H_{22}O_6$ $[M + H]^+$ 371.1495, found 371.1496.

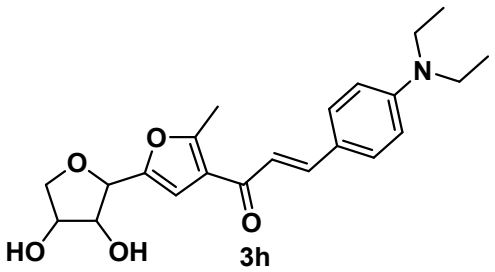

3h

Compound 3h: obtained in 89% yield; red oil; ^{1}H NMR (500 MHz, $CDCl_3$) δ 7.62 (d, *J* = 15.4 Hz, 1H), 7.42 (d, *J* = 8.6 Hz, 2H), 6.90 (d, *J* = 15.4 Hz, 1H), 6.70 (s, 1H), 6.56 (t, *J* = 9.1 Hz, 2H), 4.70 (d, *J* = 5.9 Hz, 1H), 4.35 (d, *J* = 15.7 Hz, 3H), 4.27 – 4.13 (m, 2H), 3.88 (d, *J* = 10.0 Hz, 1H), 3.34 (dd, *J* = 13.9, 6.9 Hz, 4H), 2.54 (s, 3H), 1.13 (t, *J* = 7.0 Hz, 6H). ^{13}C NMR (75 MHz, $CDCl_3$): δ 186.5, 159.0, 149.9, 149.7, 145.1, 130.9, 122.7, 121.3, 117.6, 111.2, 109.3, 76.9, 74.7, 73.1, 71.0, 44.4, 14.6, 12.5. HRMS (ESI) m/z: calcd for $C_{22}H_{27}NO_5$ $[M + H]^+$ 386.1967, found 386.1961.

6. ^{1}H NMR, ^{13}C NMR and HRMS spectra

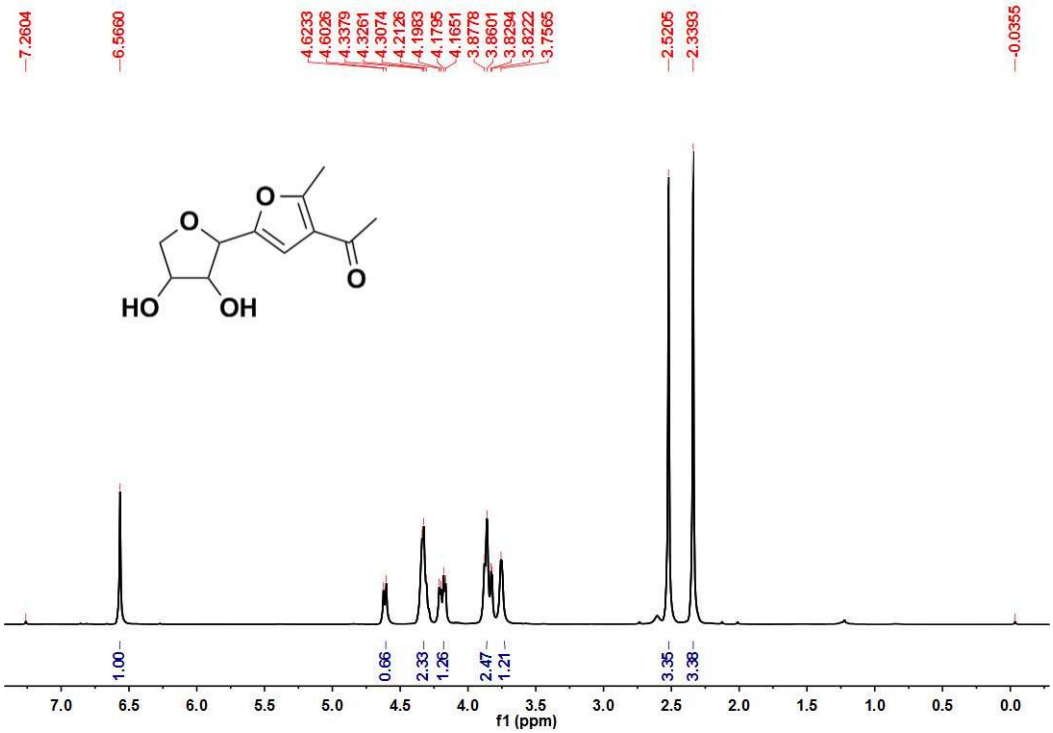

^{1}H NMR spectra of **2**

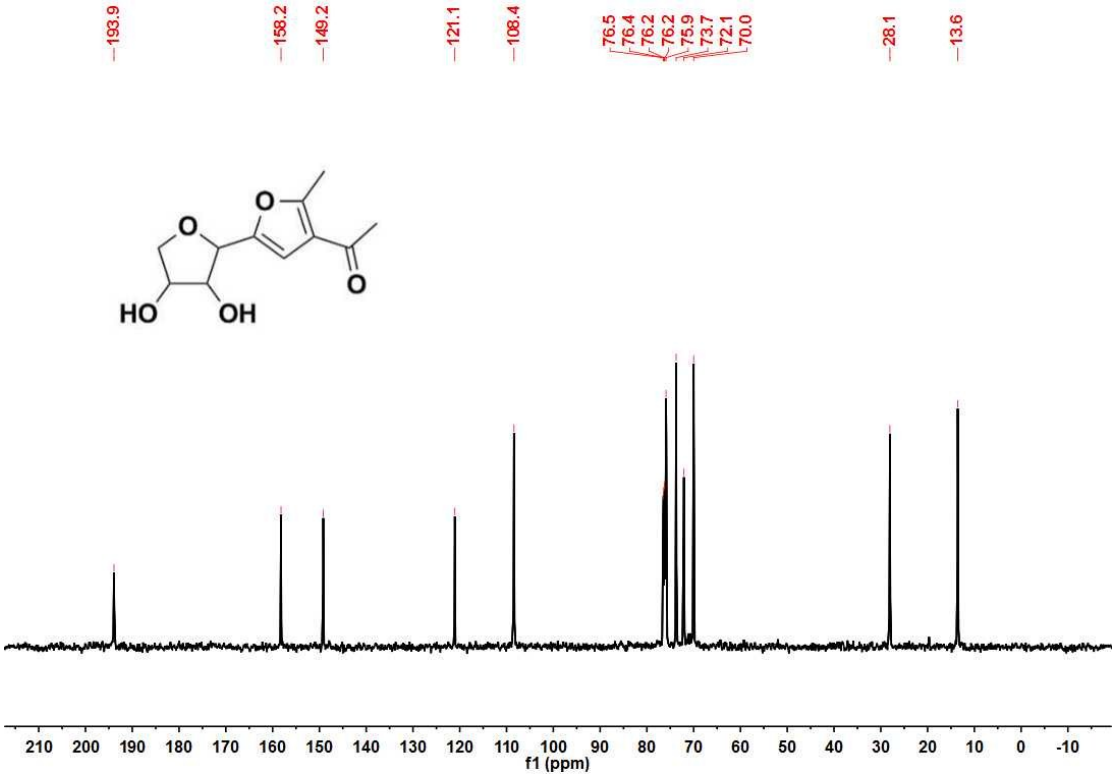

^{13}C NMR spectra of **2**

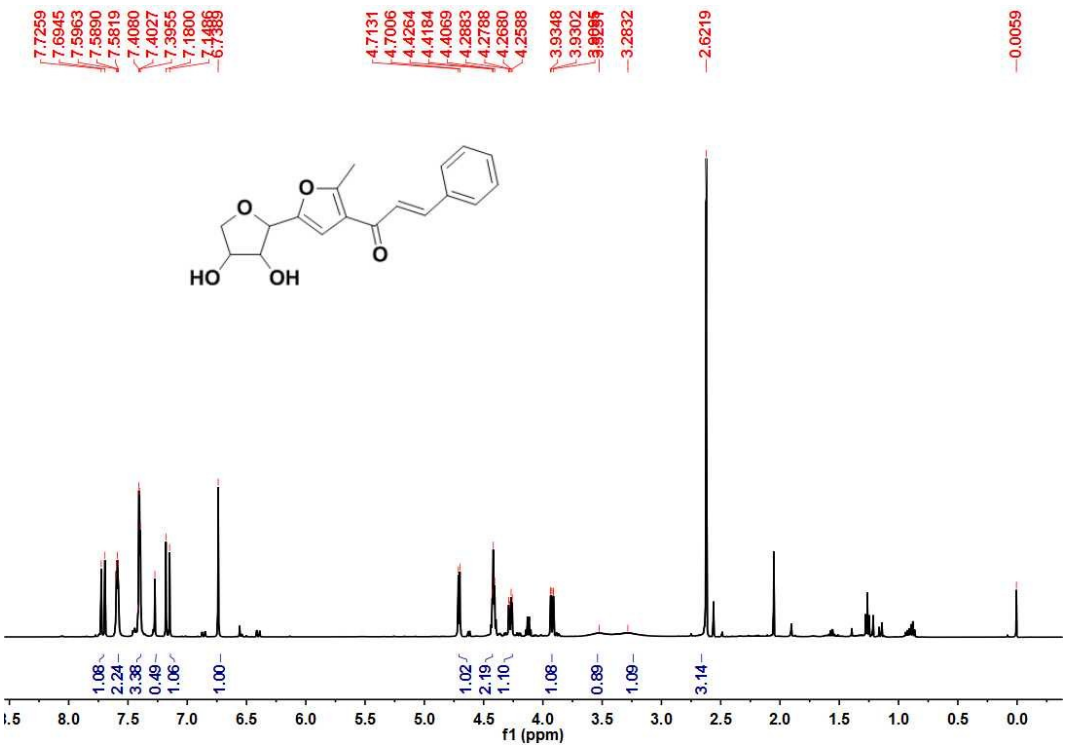

^{1}H NMR spectra of **3a**

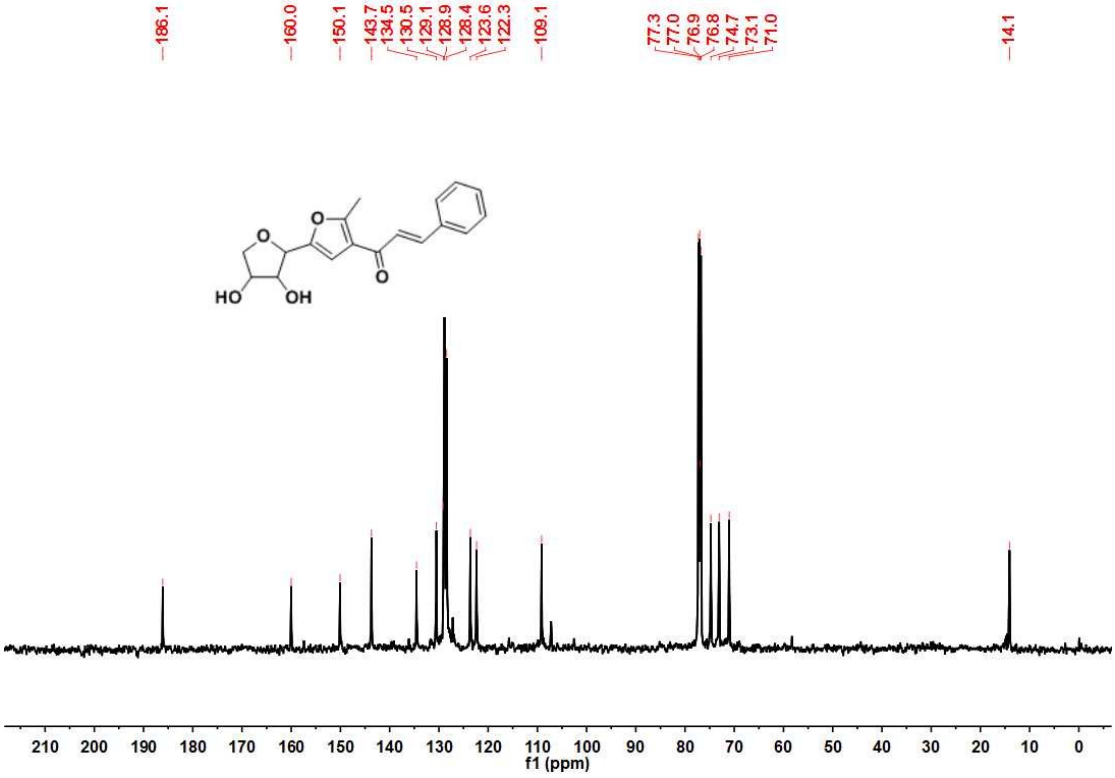

^{13}C NMR spectra of **3a**

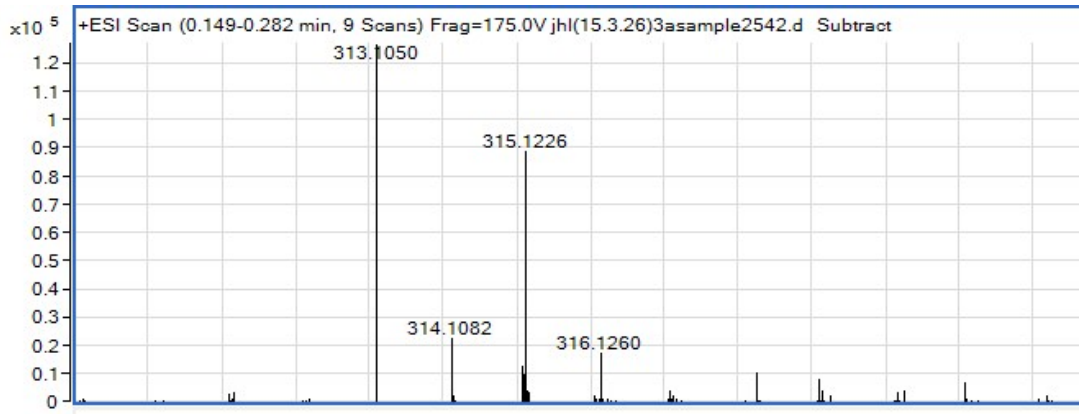

HRMS spectra of **3a**

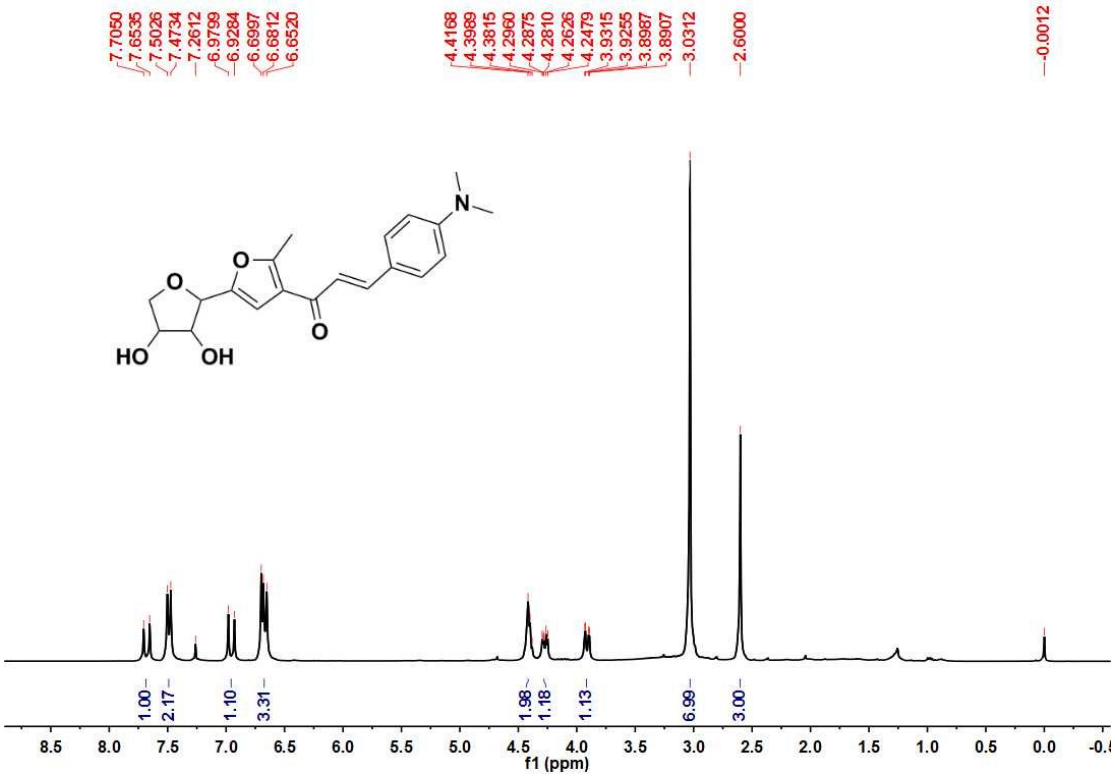

^{1}H NMR spectra of **3b**

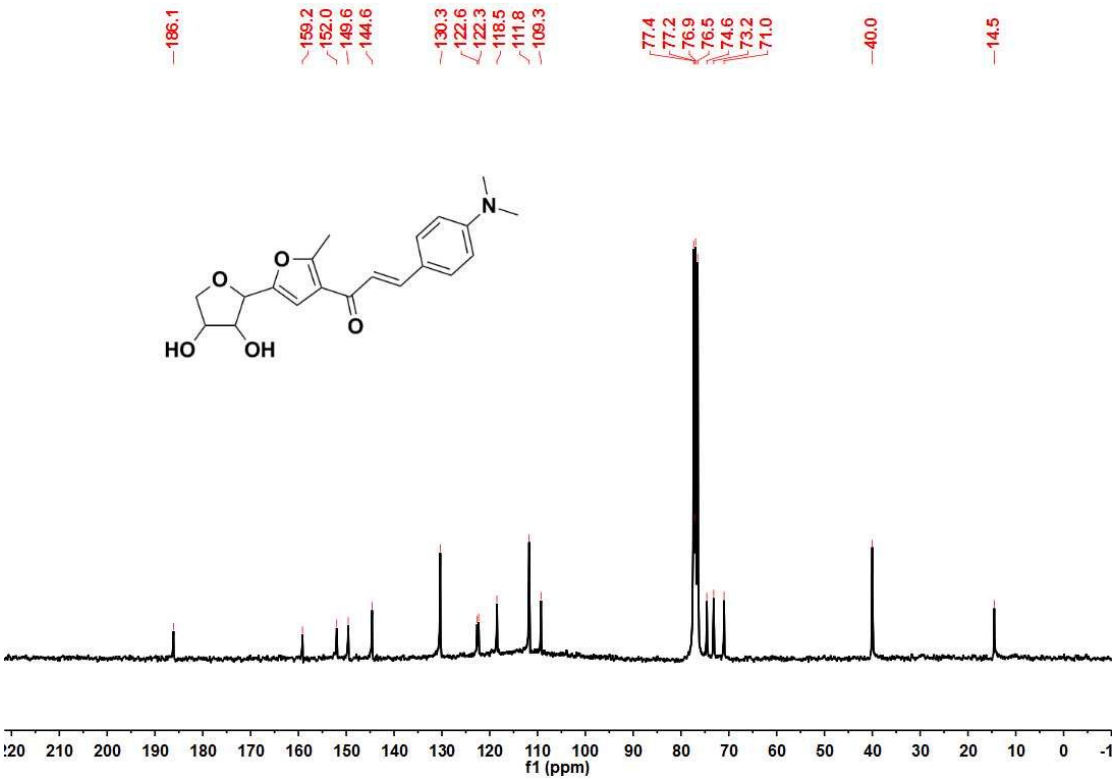

^{13}C NMR spectra of **3b**

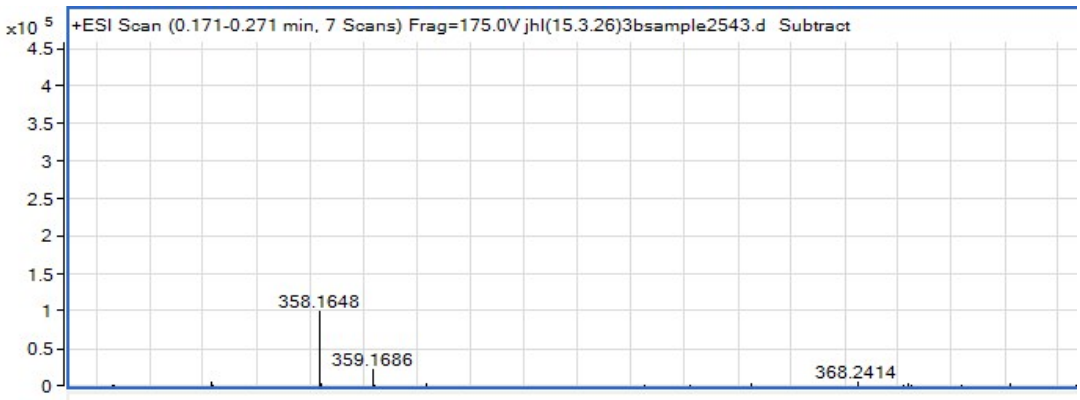

HRMS spectra of **3b**

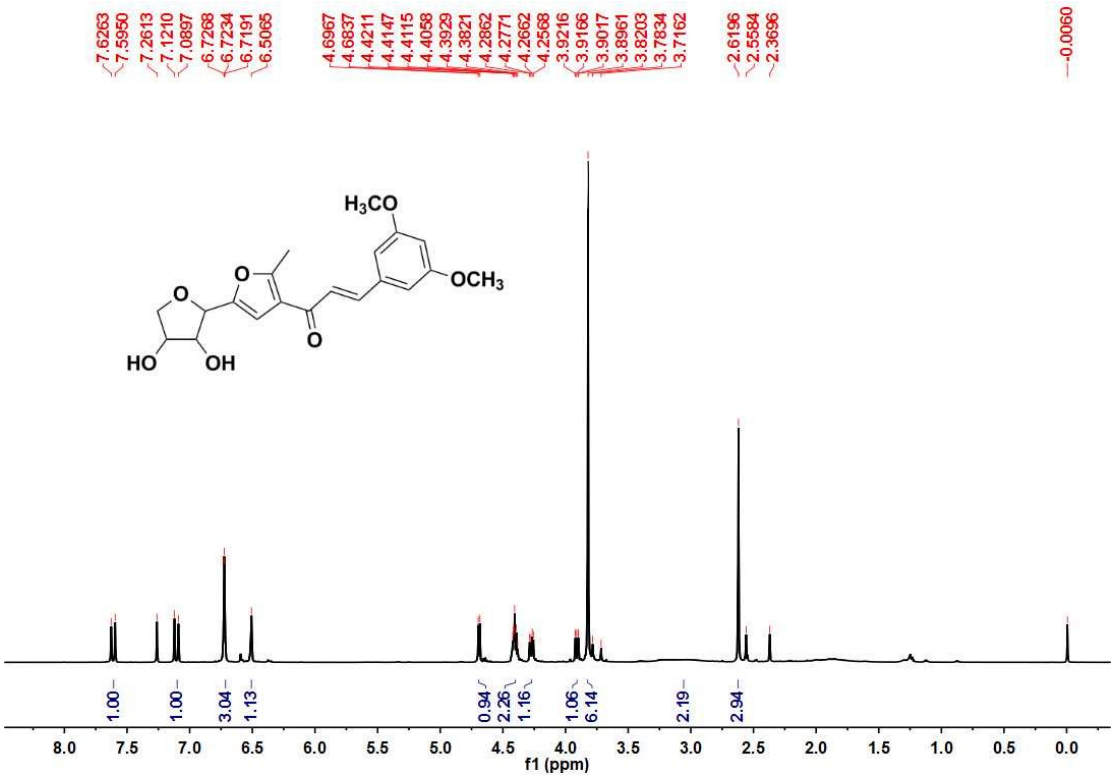

^{1}H NMR spectra of **3c**

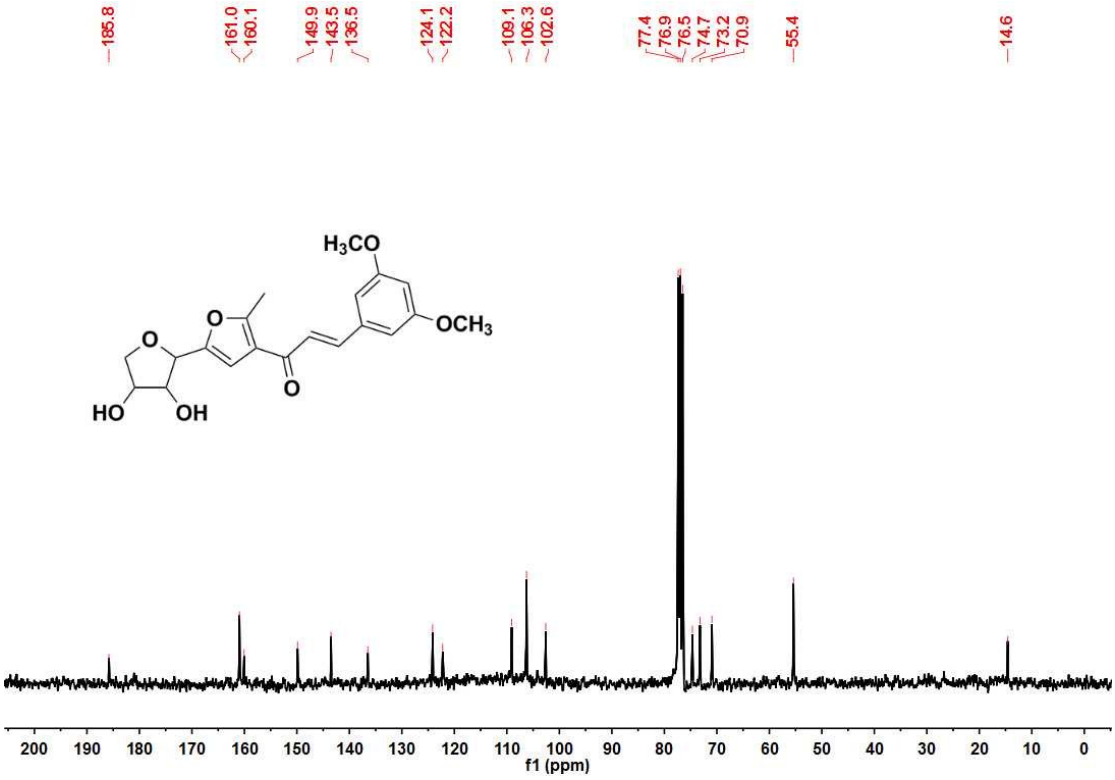

^{13}C NMR spectra of **3c**

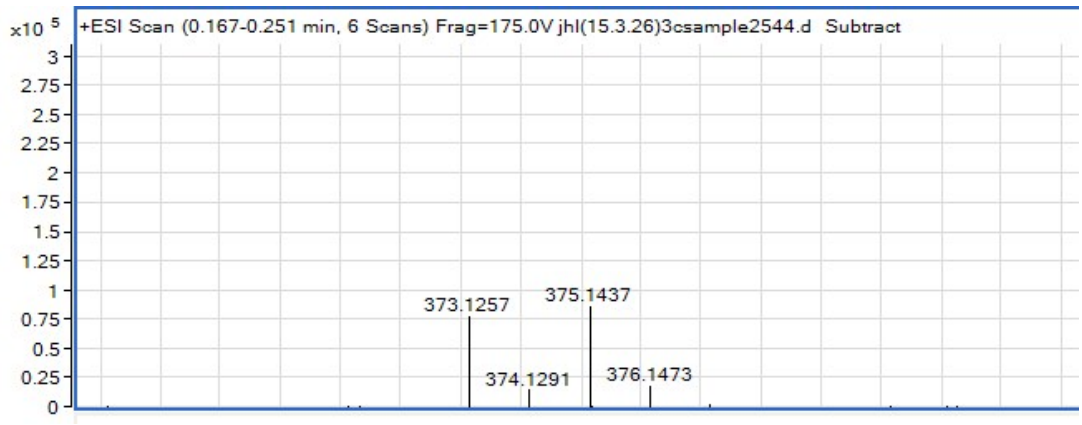

HRMS spectra of **3c**

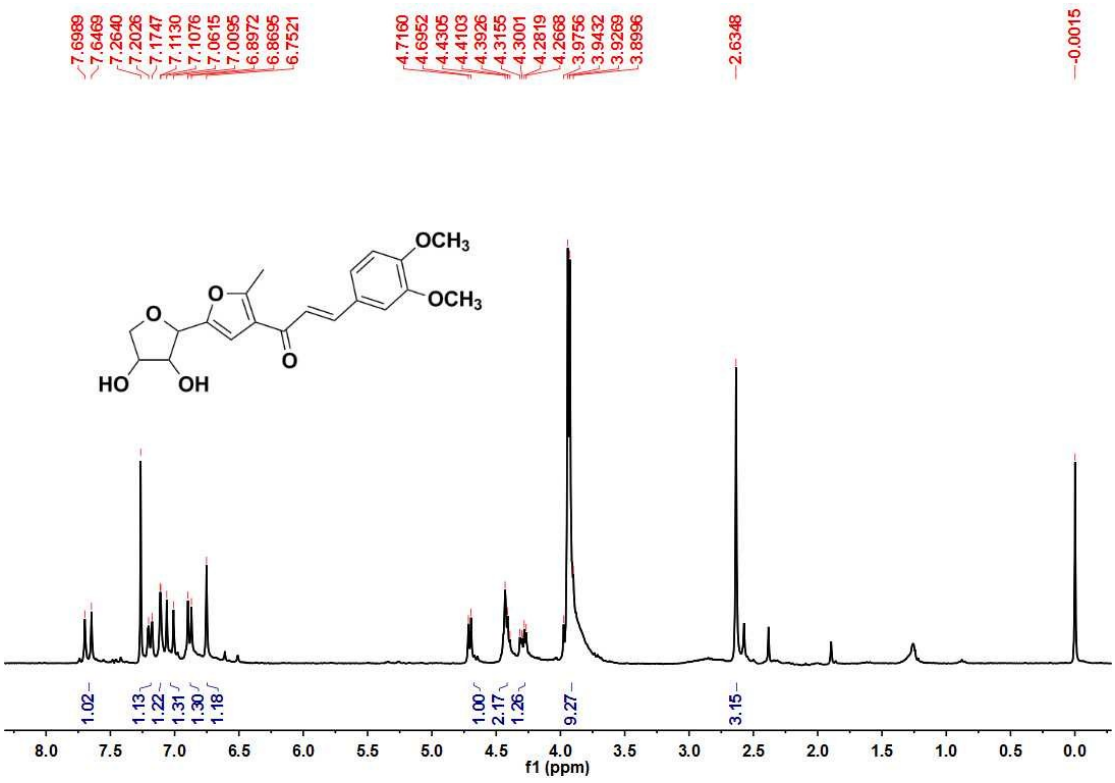

^{1}H NMR spectra of **3d**

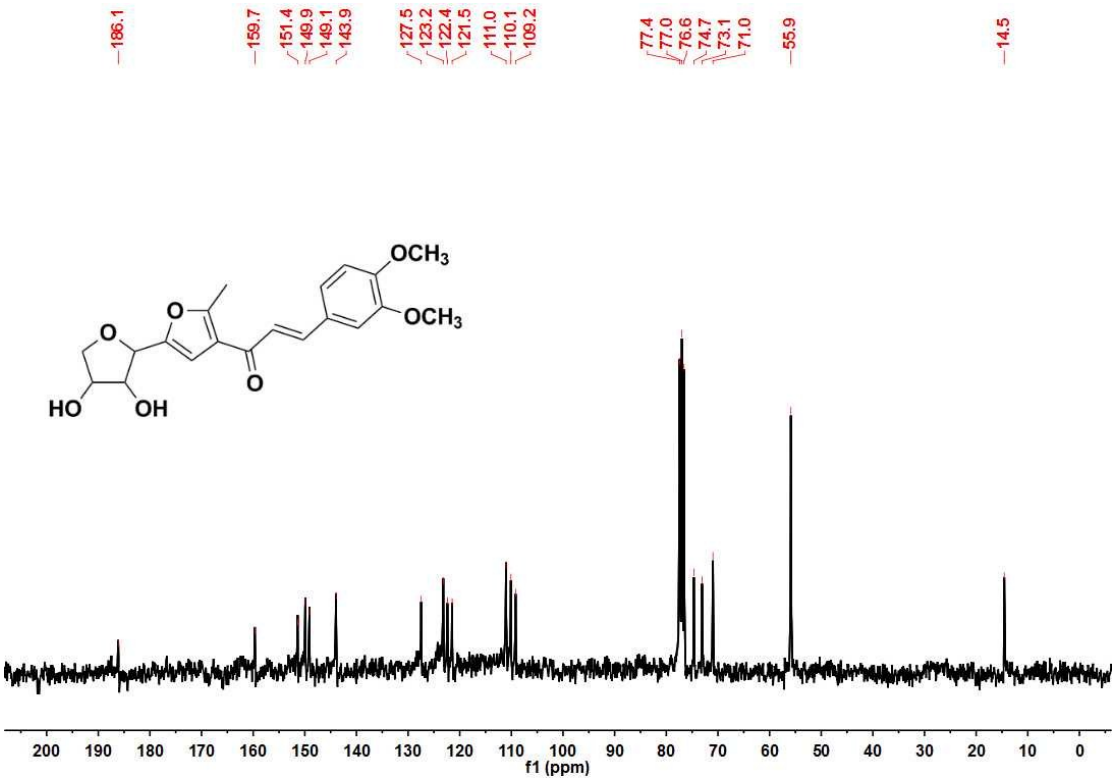

^{13}C NMR spectra of **3d**

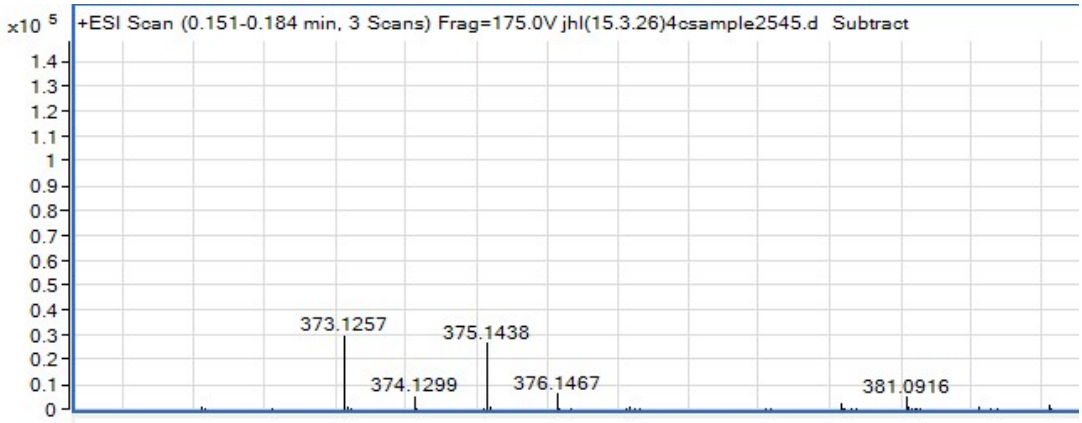

HRMS spectra of **3d**

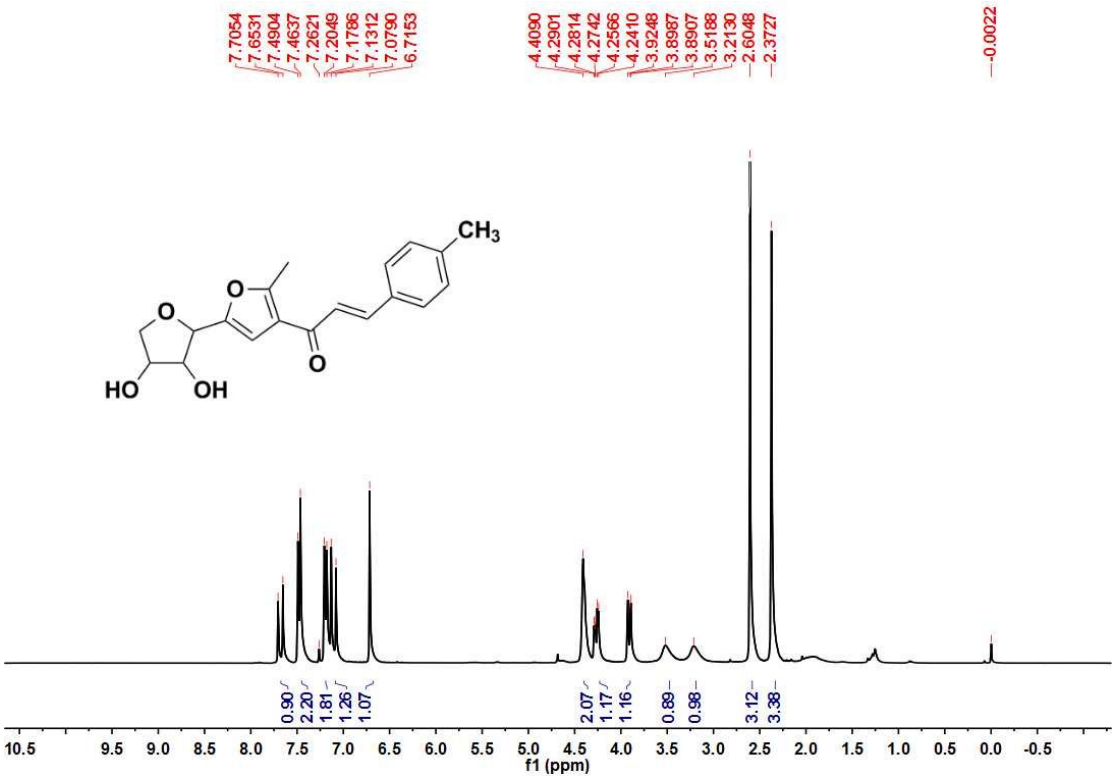

^{1}H NMR spectra of **3e**

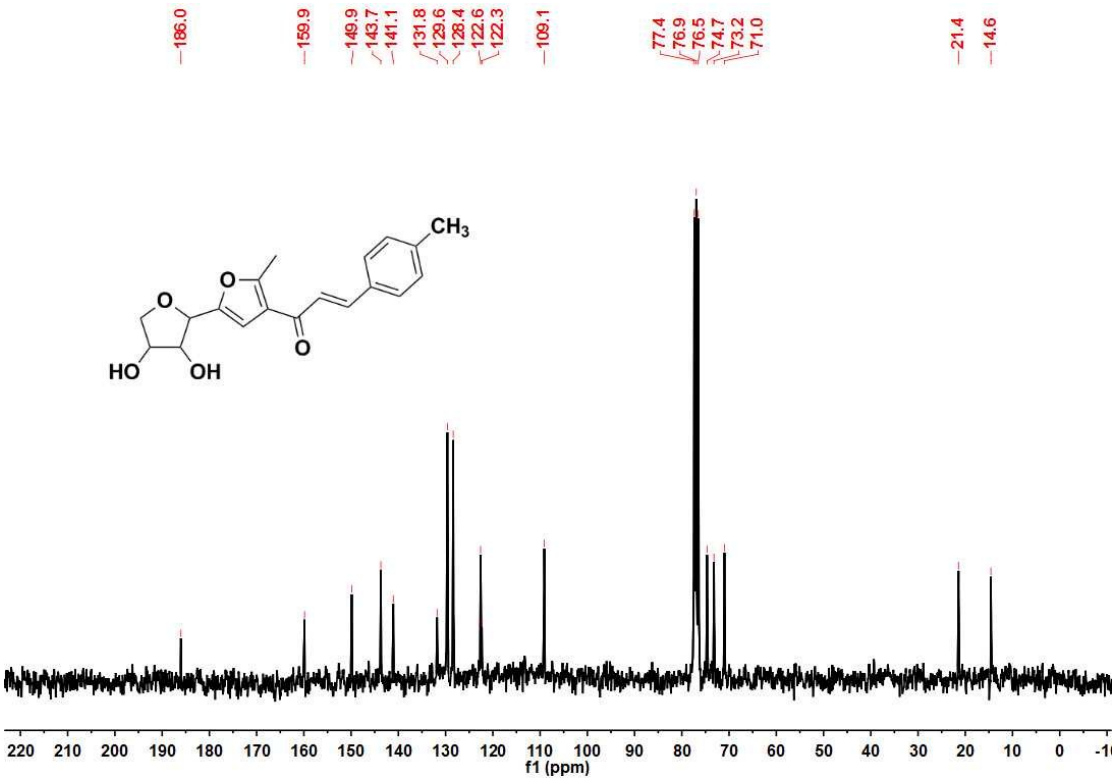

^{13}C NMR spectra of **3e**

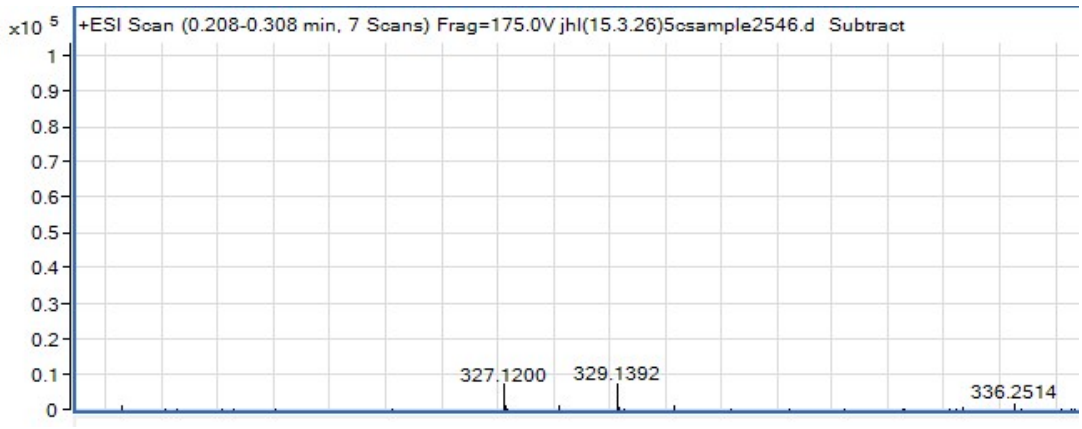

HRMS spectra of **3e**

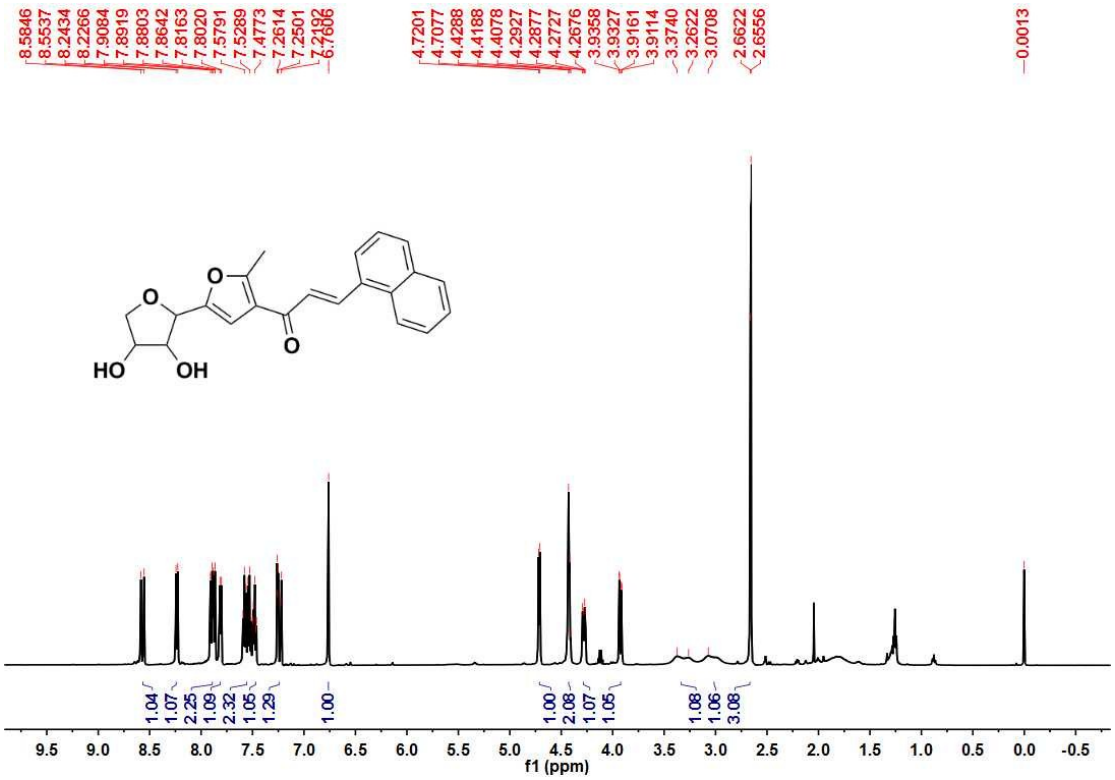

^{1}H NMR spectra of **3f**

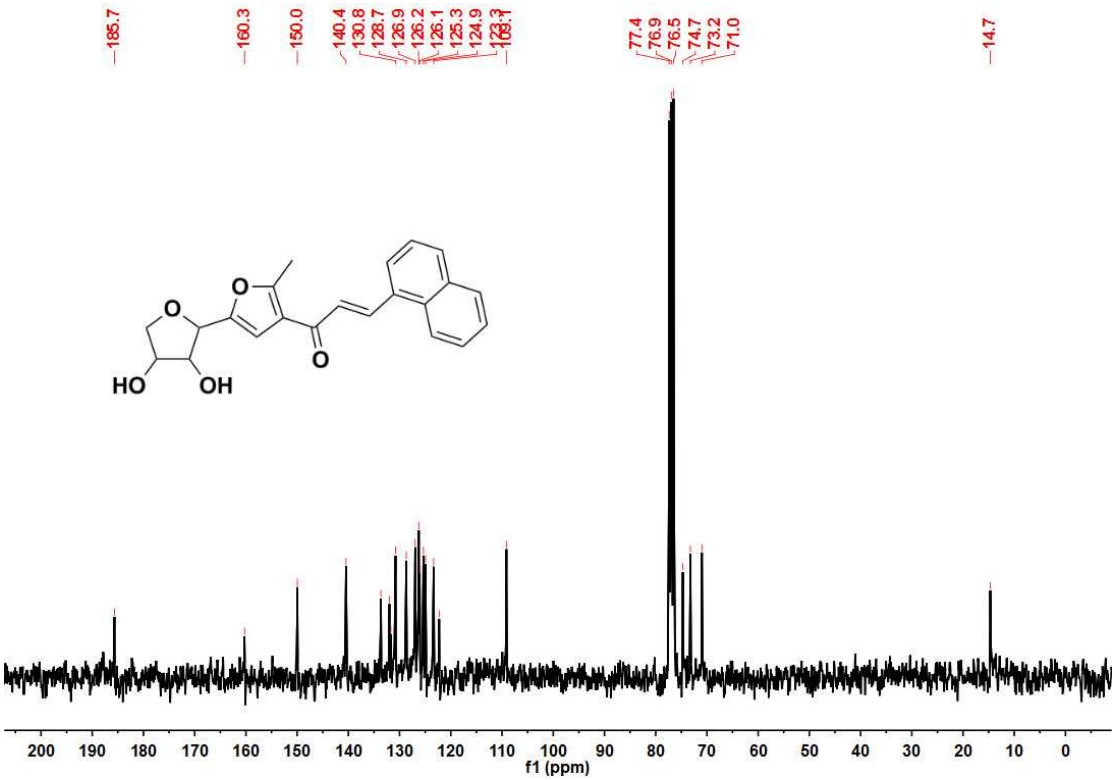

^{13}C NMR spectra of **3f**

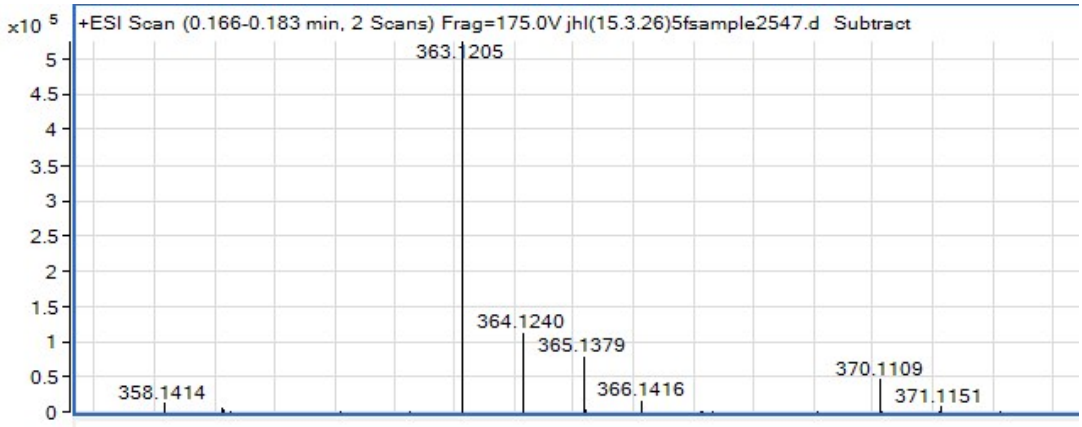

HRMS spectra of **3f**

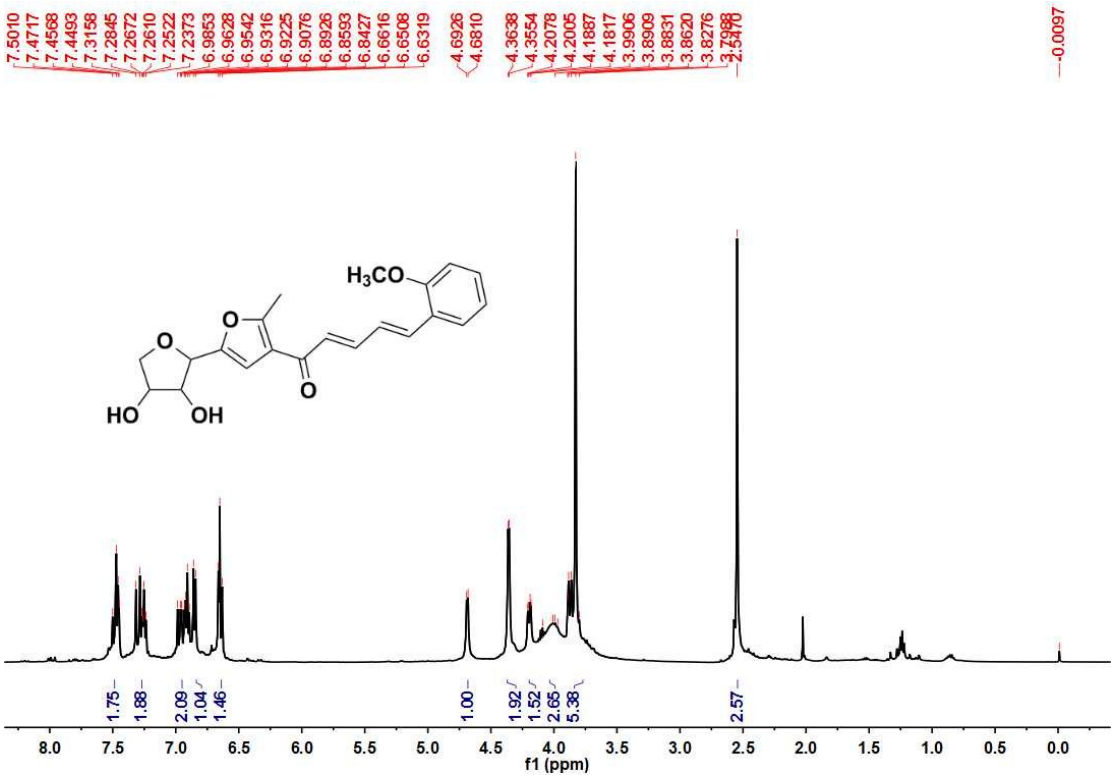

^{1}H NMR spectra of **3g**

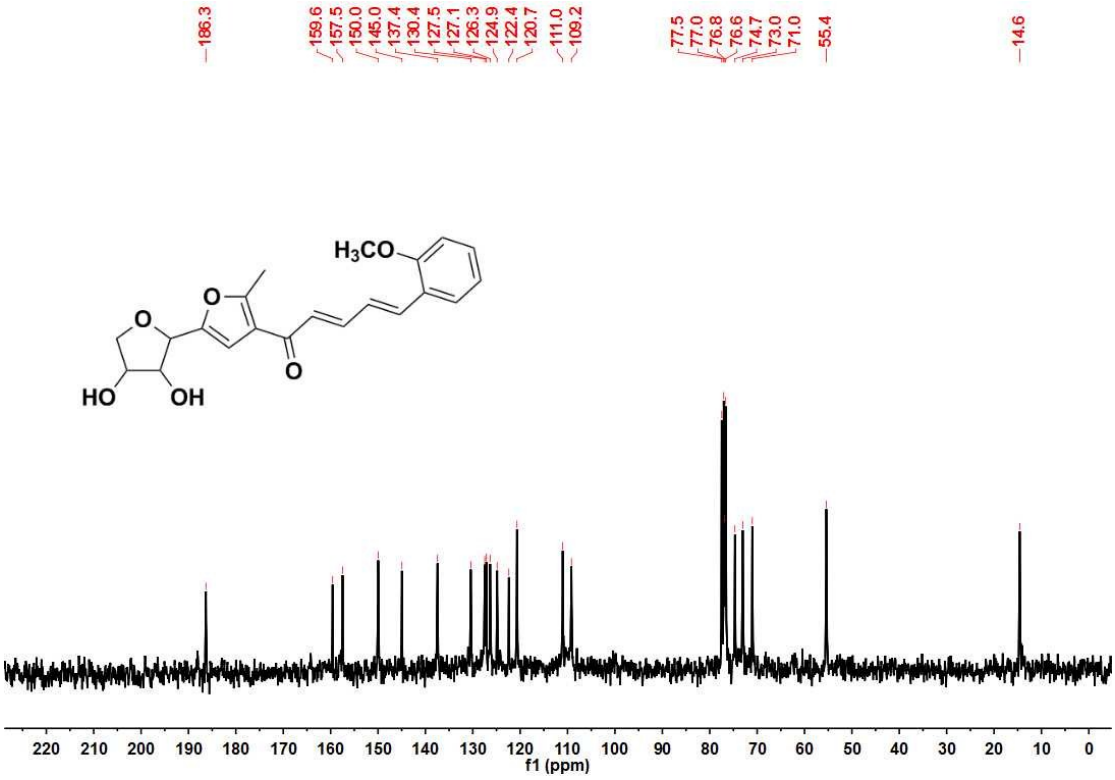

^{13}C NMR spectra of **3g**

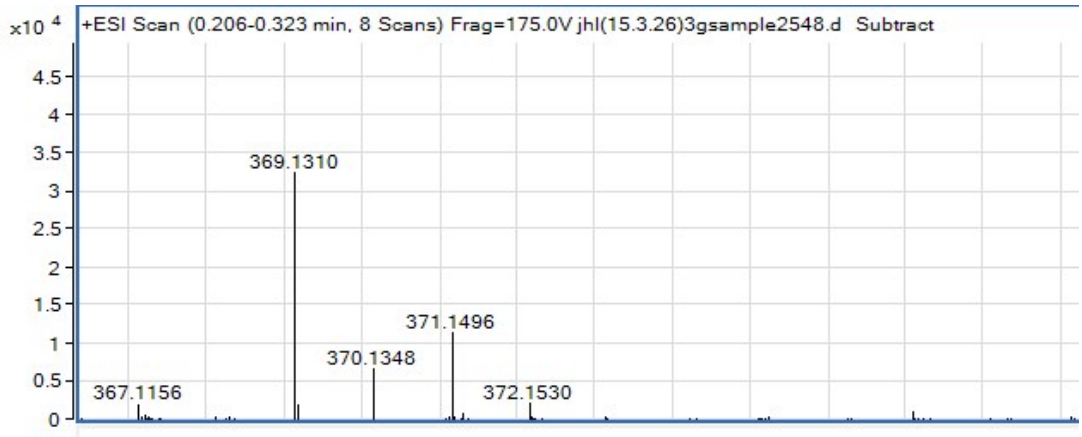

HRMS spectra of **3g**

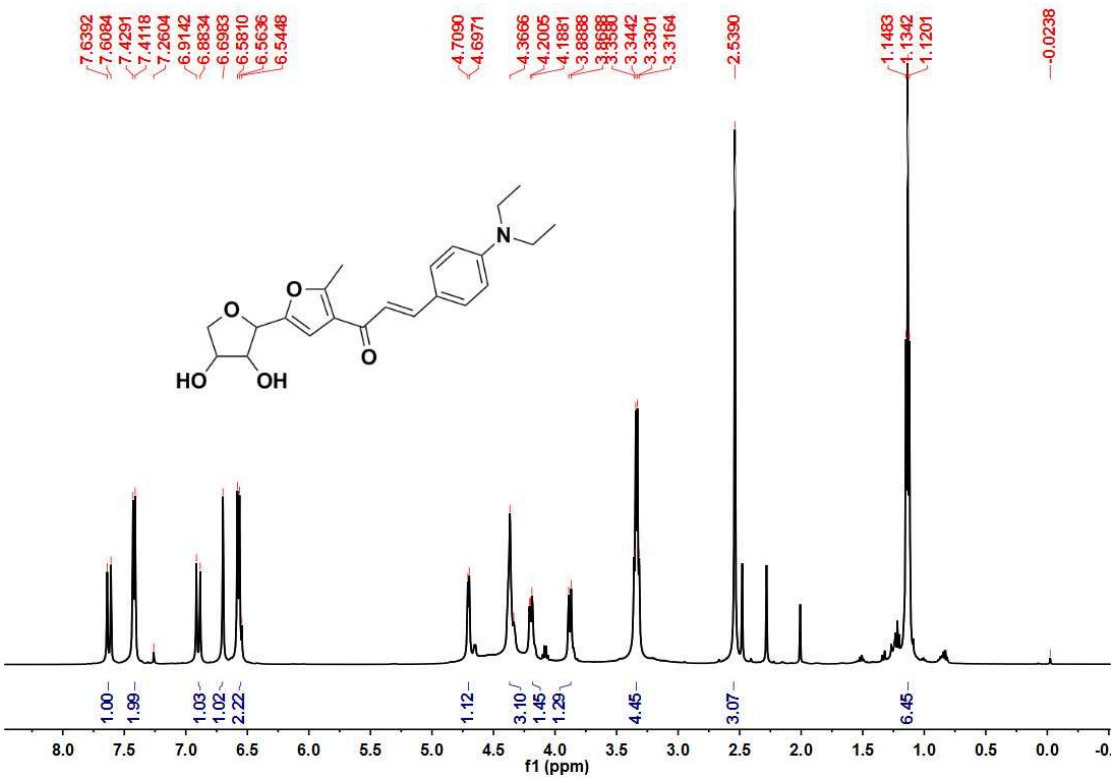

^{1}H NMR spectra of **3h**

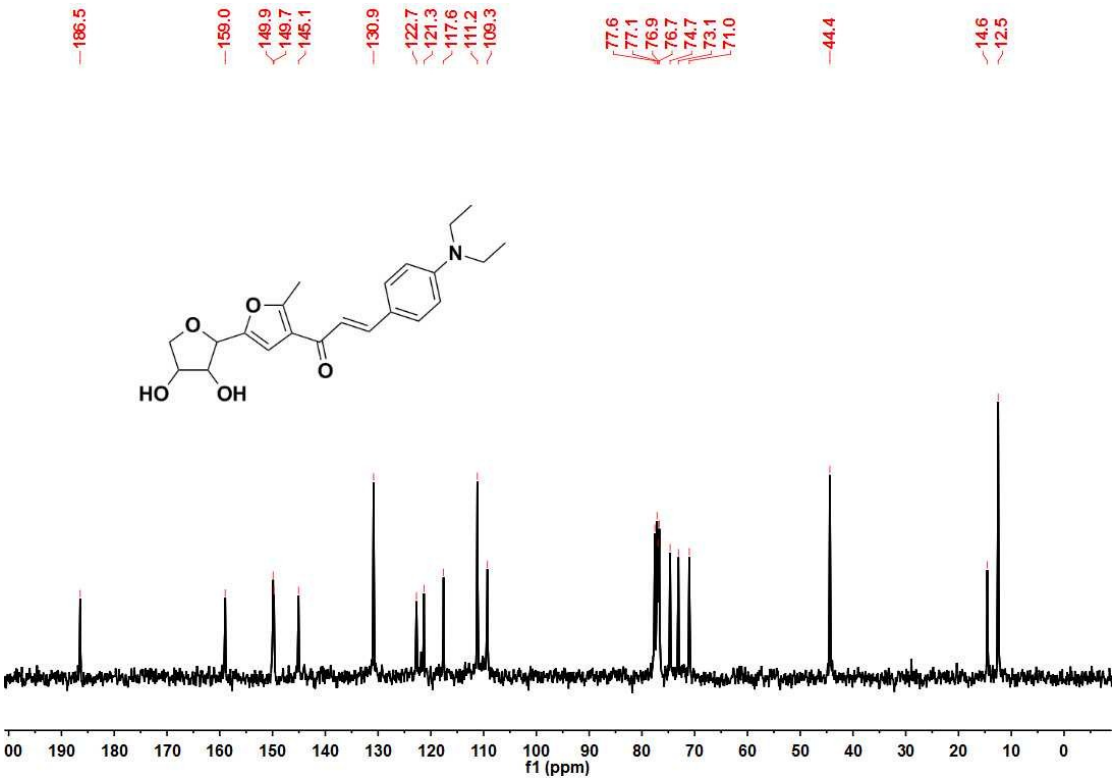

^{13}C NMR spectra of **3h**

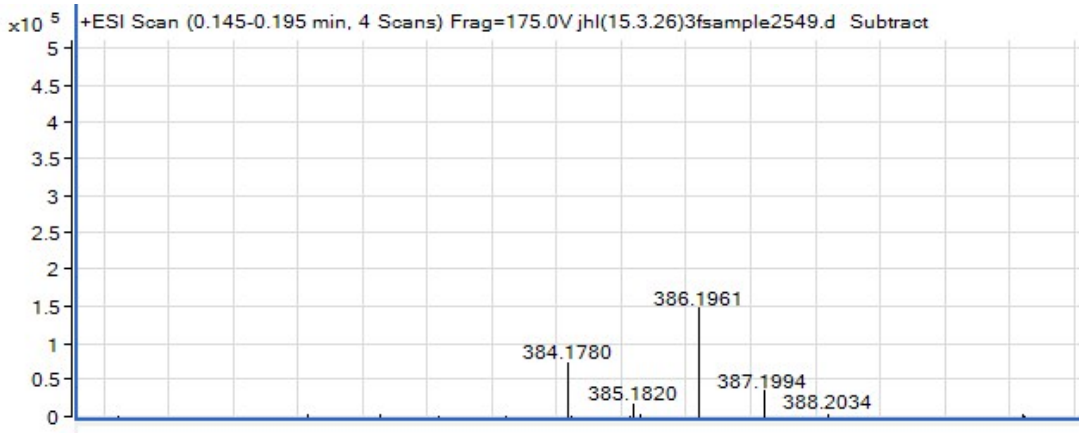

HRMS spectra of **3h**